Alkalinity sources in the Dutch Wadden Sea

Mona Norbisrath[1,2,3], Justus E. E. van Beusekom[1], & Helmuth Thomas[1,2]

[1]Institute of Carbon Cycles, Helmholtz-Zentrum Hereon, Geesthacht, 21502, Germany

[2]Institute for Chemistry and Biology of the Marine Environment (ICBM), Carl von Ossietzky University Oldenburg, Oldenburg, 26129, Germany

[3]now at: Department of Marine Chemistry and Geochemistry, Woods Hole Oceanographic Institution, Woods Hole, MA, 02543, USA

Correspondence to: Mona Norbisrath (mona.norbisrath@gmail.com)

Abstract

Total alkalinity (TA) is an important chemical property playing a decisive role in the oceanic buffering capacity of CO_2. TA is mainly generated by weathering on land, and by various anaerobic metabolic processes in water and sediments. The Wadden Sea, located in the southern North Sea is hypothesized to be a source of TA for the North Sea, but quantifications are scarce. This study shows observations of TA, dissolved inorganic carbon (DIC), and nutrients in the Dutch Wadden Sea in May 2019. Along several transects, surface samples were taken to investigate spatial distribution patterns and to compare them with data from the late 1980s. A tidal cycle was sampled to further shed light on TA generation and potential TA sources. We identified the Dutch Wadden Sea as a source of TA and estimated an export of 6.6 Mmol TA per tide to the North Sea with an average TA generation of 7.6 µmol TA kg⁻¹ h⁻¹ during ebb tide in the Ameland Inlet. TA was generated in the sediments with deep pore water flow during low tide enriching the surface water. A combination of anaerobic processes and $CaCO_3$ dissolution were potential TA sources of TA in the sediments. We deduce that seasonality and the associated nitrate availability in particular influence TA generation by denitrification, which is low in spring and summer.

1 Introduction

As the regulator of the ocean carbon dioxide (CO_2) sink, total alkalinity (TA) is of increasing scientific interest and is investigated worldwide in the so called "Anthropocene" (Abril and Frankignoulle, 2001;Bozec et al., 2005;Chen and Wang, 1999;Dickson, 1981;Middelburg et al., 2020;Norbisrath et al., 2022;Renforth and Henderson, 2017;Thomas et al., 2004;2009;Sabine et al., 2004). The "Anthropocene" describes the current era of our planet, when environmental changes, driven by humans, have become identifiable in geological records (Zalasiewicz et al., 2010;Crutzen, 2002). One of the most threatening changes for our climate is the anthropogenic driven increase in atmospheric greenhouse gases (GHG), such as CO_2. To counteract the increasing atmospheric CO_2 concentrations and the ongoing climate warming, a combination of several pathways is needed. Beside a strict reduction of CO_2 emissions, also net-negative emissions are required, which capture the

atmospheric CO_2 and store it either based on land or in the ocean (e.g., Keith et al., 2006;Matthews and Caldeira, 2008;Zhang et al., 2022). The climate and the increasing atmospheric CO_2 content is also naturally regulated by the open ocean, and around a quarter of the global anthropogenic CO_2 emissions are already removed by it (Friedlingstein et al., 2022). The carbon storage capacity of the North Sea is an important atmospheric CO_2 sink as it exports the absorbed CO_2 in the deep layers of the Atlantic Ocean where it is stored on longer time scales (Borges et al., 2005;Bozec et al., 2005;Burt et al., 2016;Brenner et al., 2016;Hu and Cai, 2011;Schwichtenberg et al., 2020;Thomas et al., 2004;2009). Two important aspects of the oceanic climate regulation are the oceanic circulation and TA. TA, primarily consisting of bicarbonate and carbonate, is generated by chemical rock weathering (Suchet and Probst, 1993;Meybeck, 1987;Berner et al., 1983), and in various stoichiometries by calcium carbonate ($CaCO_3$) dissolution and anaerobic metabolic processes, such as denitrification, which is the reduction process of nitrate to dinitrogen gas in the nitrogen cycle (Hu and Cai, 2011;Wolf-Gladrow et al., 2007;Chen and Wang, 1999;Brewer and Goldman, 1976). Since TA, CO_2 uptake and its export to the deep ocean are mainly disentangled in the open ocean, TA and the oceanic circulation interact closely in highly active and shallow ocean areas such coastal zones and continental and marginal shelves. In these shallow areas, TA is susceptible to changes due to various metabolic processes and the influence of adjacent zones like rivers, estuaries, marshes, and tidal flats (e.g., Norbisrath et al., 2022;2023;Wang et al., 2016;Voynova et al., 2019). A previous study by Norbisrath et al. (2022) showed that an enhanced riverine, metabolic alkalinity would lead to increasing CO_2 absorption in the coastal zones of the North Sea, highlighting the need to further investigate TA regulation in adjacent zones of coastal oceans.

Coastal zones, which are the direct interface between most, if not all, compartments of the Earth system (i.e., atmospheric, terrestrial, aquatic, and oceanic) and human societies, appear particularly vulnerable to environmental and climate change (Glavovic et al., 2015). This holds true for the Wadden Sea, the shallow, coastal sea along an approximately 500 km coastline of the Netherlands, Germany, and Denmark, in the southern North Sea, which is declared as an UNESCO world natural heritage site since 2009. Most of the Wadden Sea is located between the protecting barrier Islands and the Mainland, which makes it the world's largest uninterrupted stretch of tidal flats with multiple tidal inlets (Fig. 1). Due to the topography, the Wadden Sea is a highly dynamic ecosystem with influences from the mainland and the North Sea (Hoppema, 1993;Postma, 1954;van Raaphorst and van der Veer, 1990). Driving forces of the biogeochemical dynamics in the Wadden Sea are nutrient imports by rivers and high suspended particulate matter (SPM) and organic matter (OM) imports from the North Sea (van Beusekom et al., 2019;van Beusekom et al., 2012;Postma, 1954). Physical sources of variability in the Wadden Sea are oceanic driven wind, waves, and tidal currents, as well as the counterclockwise circulation of the North Sea (Elias et al., 2012). Large tidal amplitude and currents in conjunction with shallow water depths allow for vertical water column mixing and an exchange between the pelagic and benthic realms including deep pore water exchange (Røy et al., 2008). The strong tidal currents also impact the biogeochemistry of the North Sea (Postma, 1954), as they cause an exchange of water between the North Sea and the Wadden Sea and play an important role in the import of particulate matter from the North Sea (Burchard et al., 2008).

Previous studies identified the Wadden Sea as a TA source for the North Sea with a loading between 39 Gmol yr^{-1} (Schwichtenberg et al., 2020) and 73 Gmol yr^{-1} (Thomas et al., 2009). Both studies suggested the entire Wadden Sea as one of

64 the most important TA sources of the carbon storage capacity for the North Sea. Burt et al. (2016) highlighted the importance

65 of coastal TA production for regulating the buffer system in the North Sea, and suggested denitrification as the major TA

66 source. Due to the strong connection between the North Sea and the Wadden Sea, a better understanding of TA generation in

67 the latter is required. Here, we focus on the Dutch Wadden Sea that has been well-studied during the past decades (Hoppema,

68 1990, 1991, 1993;De Jonge et al., 1993;Elias et al., 2012;Ridderinkhof et al., 1990;Postma, 1954;van Beusekom et al.,

69 2019;Schwichtenberg et al., 2017). In particular Hoppema (1990);(1993) observed the spatial and temporal variability of TA

70 in May in the late 1980s, which we compare with our observed transect data to detect potential differences over the last 30

71 years. In addition, we further discussed potential TA sources in the Dutch Wadden Sea.

72 2 Methods

73 2.1 Study site and sampling

74 This study is based on samples collected on a research cruise (LP20190515) in the Dutch Wadden Sea (Frisian Islands) on RV

75 *Ludwig Prandtl* in May 2019 (Fig. 1). We collected water samples in the Wadden Sea starting at Harlingen, through the Vlie

76 Inlet along the islands Vlieland and Terschelling, through the Ameland Inlet to Ameland Island, from there on via the Frisian

77 Inlet to Lauwersoog, and around Schiermonnikoog Island via the Ems-Dollard Inlet to Emden. In addition, we sampled a half

78 tidal cycle during ebb tide (from high tide to low tide) on 21 May 2019. To set the range of ebb tide data in relation, we also

79 sampled a half tidal cycle during flood tide (from low tide to high tide) on 23 May 2019 for comparison. Both half tidal cycles

80 were sampled as an anchor station in the waterway at the western side of Ameland in the Ameland Inlet on each day.

81 Nearly half-hourly, we collected discrete surface (1.2 m depth) water samples with a bypass from the onboard flow-through

82 FerryBox system, (Petersen et al., 2011), which also provided essential physical parameters such as salinity with an accuracy

83 of 0.02 (PSU) and temperature with an accuracy of 0.1 °C (Petersen et al., 2011). The FerryBox was cleaned and the system

84 checked prior to the cruise, and salinity is occasionally checked using discrete samples, which is considered sufficient for

85 gradients in near-shore investigations (pers. comm. Y. Voynova). We complemented our salinity and temperature data with

86 data from three Rijkswaterstaat stations (Dantziggat, Terschelling 10, and Vliestroom; Table B3), which were close to our

87 stations.

88 For TA and DIC measurements we sampled water with overflow into 300 mL BOD (biological oxygen demand) bottles and

89 preserved them with 300 µL saturated mercury chloride solution ($HgCl_2$) to stop biological activity. Each BOD bottle was

90 filled without air bubbles and closed by using a ground-glass stopper coated in Apiezon® type M grease and a plastic cap. The

91 samples were stored in a cool dark environment until measurements in the lab.

92 Water for nutrient samples was filtered through pre-combusted (4 h, 450 °C) GF/F filters and the filtrate was stored frozen in

93 three 15 mL Falcon tubes for triplicate measurements in the lab.

94 To determine the total carbon (C), organic carbon (C_{org}) and nitrogen (N) concentrations in SPM and associated C_{org}:N ratios,

95 we used pre-combusted (4 h, 450 °C) GF/F filters, which were dried after sampling at 50 °C to remove all humidity and were

96 stored frozen afterwards until measurement.
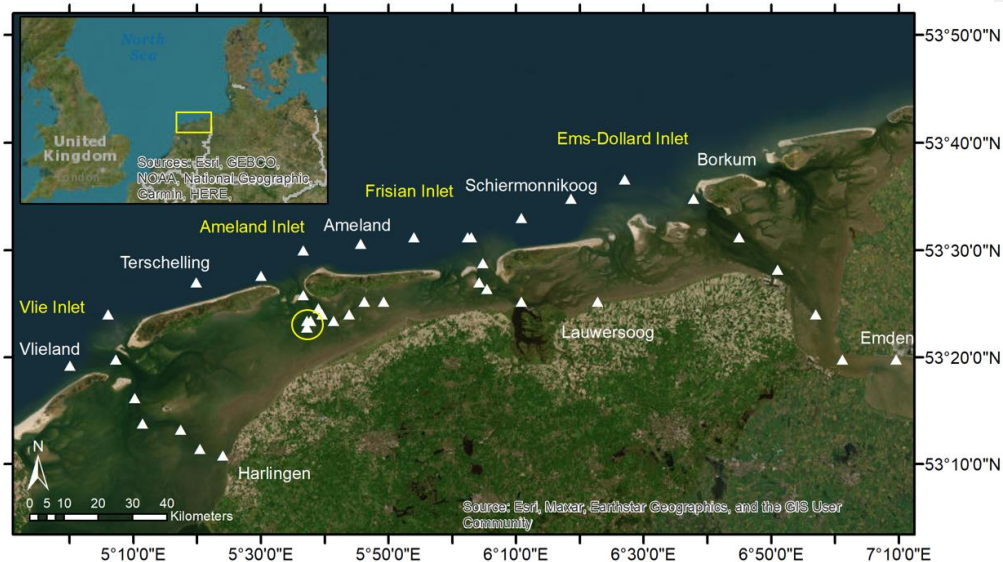
97

98 **Figure 1** Sampling site in the Dutch Wadden Sea. The sampling stations around the Frisian Islands in May 2019 are visualized

99 with white triangles. The yellow circle highlights the anchor stations for the tidal cycle sampling in the Ameland Inlet on two

100 days. During the sampling day from low tide to high tide, we had two samples that we took slightly more western due to

101 drifting. The island and city names are shown in white, the inlets in yellow. The tidal flats and sedimentary structures are well

102 visible between the barrier islands and the mainland.

103 **2.2 Carbon species analyses**

104 The parallel analyses of TA and DIC were carried out in March 2020 by using the VINDTA 3C (Versatile INstrument for the

105 Determination of Total dissolved inorganic carbon and Alkalinity, MARIANDA - marine analytics and data), which measures

106 TA by potentiometric titration and DIC by coulometric titration both with a measurement precision < 2 µmol kg^{-1} (Shadwick

107 et al., 2011). Certified reference material (CRM batch # 187) provided by Andrew G. Dickson (Scripps Institution of

108 Oceanography) was measured before and after the samples and used to ensure a consistent calibration of both measurements.

109 The calcite and aragonite saturation states (Ω), and the pH, and the seawater partial pressure of CO_2 (pCO_2) were computed

110 with the CO_2SYS program (Lewis and Wallace, 1998), using the measured parameters TA and DIC, and salinity, temperature,

111 silicate and phosphate as input variables, together with the dissociation constants from Mehrbach et al. (1973), as refit by

112 Dickson and Millero (1987). Reported calculation uncertainties are ± 0.0062 for pH (Millero et al., 1993), ± 4.9 % for the

113 aragonite saturation state and ± 3.5 % for pCO$_2$ (Orr et al., 2018).

114 **2.3 Nutrient analyses**

115 The nutrients were measured with a continuous flow automated nutrient analyzer (AA3, SEAL Analytical) and a standard

116 colorimetric technique (Hansen and Koroleff, 2007) for nitrate (NO_3^-), nitrite (NO_2^-), phosphate (PO_4^{3-}), and silicate (Si), and

117 a fluorometric method (Kérouel and Aminot, 1997) for ammonium (NH_4^+) (Grasshoff et al., 2009). The nutrient samples were

118 measured against Eurofins reference materials VKI SW4.1B (for NOx, NO$_2$ and NH$_4$) and VKI SW4.2B (for Si and PO$_4$) in

119 July 2019. The maximum standard deviations were 0.322 µmol L^{-1} for NO_3^-, 0.014 µmol L^{-1} for NO_2^-, 0.081 µmol L^{-1} for

120 NH_4^+, 0.014 µmol L^{-1} for PO_4^{3-} and 0.165 µmol L^{-1} for Si.

121 For the C$_{org}$ determination, filters were acidified with 1N HCl and dried overnight to remove all inorganic carbon content.

122 Filters were measured with a CHN-elemental analyzer (Eurovector EA 3000, HEKAtech GmbH) in the Institute of Geology,

123 University Hamburg, and calibrated against a certified acetanilide standard (IVA Analysentechnik, Germany). The standard

124 deviations were 0.05 % for carbon and 0.005 % for nitrogen.

125 **2.4 Data analyses**

126 The data analyses were performed by using RStudio Version 1.3.1073 © 2009-2020 RStudio, PBC. The linear regression

127 Model II was performed by using the "lmodel2" R package, and the plots were created with the "ggplot2" R package.

128 **3 Results**

129 **3.1 Spatial parameter distribution**

130 To investigate the spatial distribution of TA in the Dutch Wadden Sea and compare its general status with earlier studies (in

131 particular Hoppema, 1990), we observed TA and related parameters in surface water along a transect from the coastal mainland

132 towards the North Sea.

133 The temperatures varied between 12 and 16 °C with higher temperatures towards the coastal mainland (Fig. 2a). We identified

134 two main sub regions based on the salinity values. First the Ems-Dollard Inlet, which showed salinities lower than 28 and with

135 the minimum value of 20.25 at the most upstream station. And second, around Ameland Island and the remaining of our

136 investigated region in the Dutch Wadden Sea with salinities showing only smaller minor variationsdifferences varying from

137 28 to 33 (Fig. 2b).

138 Spatial transect TA concentrations ranged from 2332 µmol TA kg^{-1} to 2517 µmol TA kg^{-1}. We observed lower concentrations

139 on the North Sea side of the Frisian Islands with somewhat higher concentrations around Ameland (Fig. 2c). In contrast to the

140   North Sea side, the values were higher (> 2380 µmol TA kg^{-1}) in the Wadden Sea. In the Ems-Dollard Inlet, the concentrations

141   were even higher, with values up to 2517 µmol TA kg^{-1} at the most upstream station.

142   Silicate (Si) showed higher concentrations in the Wadden Sea and lower ones towards the North Sea (Fig. A1a). Highest

143   concentrations were observed at the coastal mainland and in the Ems-Dollard Inlet. Silicate concentrations ranged between 0.3

144   and 56.3 µmol Si L^{-1}. Both, the calcite and aragonite saturation states (Ω) were supersaturated in the entire study region.

145   Saturation state values ranged from 2.3 to 4.6 for calcite (Fig. A1b), and from 1.4 to 2.8 for aragonite (Table B3). Highest

146   values were observed at the North Sea side of the barrier islands, and lowest values near Harlingen and in the Ems-Dollard

147   Inlet. Like the calcite and aragonite saturation states, the pH values were higher in the North Sea, and lower in the Wadden

148   Sea and near the coastal mainland (Fig. A1c). The pH values ranged from 7.86 to 8.19, and lowest values were observed near

149   Harlingen and in the Ems-Dollard Inlet. The nitrate (NO_3^-) concentrations were in a low range (< 3 µmol NO_3^- L^{-1}) throughout

150   the study region. Higher concentrations (< 6 µmol NO_3^- L^{-1}) were observed only at a few stations close to land, and maximum

151   concentrations (< 38 µmol NO_3^- L^{-1}) were observed in the Ems-Dollard Inlet (Fig. A1d). DIC concentrations ranged from 2097

152   µmol DIC kg^{-1} to 2430 µmol DIC kg^{-1} (Fig. A1e). DIC values showed a similar pattern as TA values, with higher concentrations

153   near the coastal mainland and in the Ems-Dollard Inlet, and decreasing concentrations toward the North Sea, where DIC

154   reached minimum values.

155
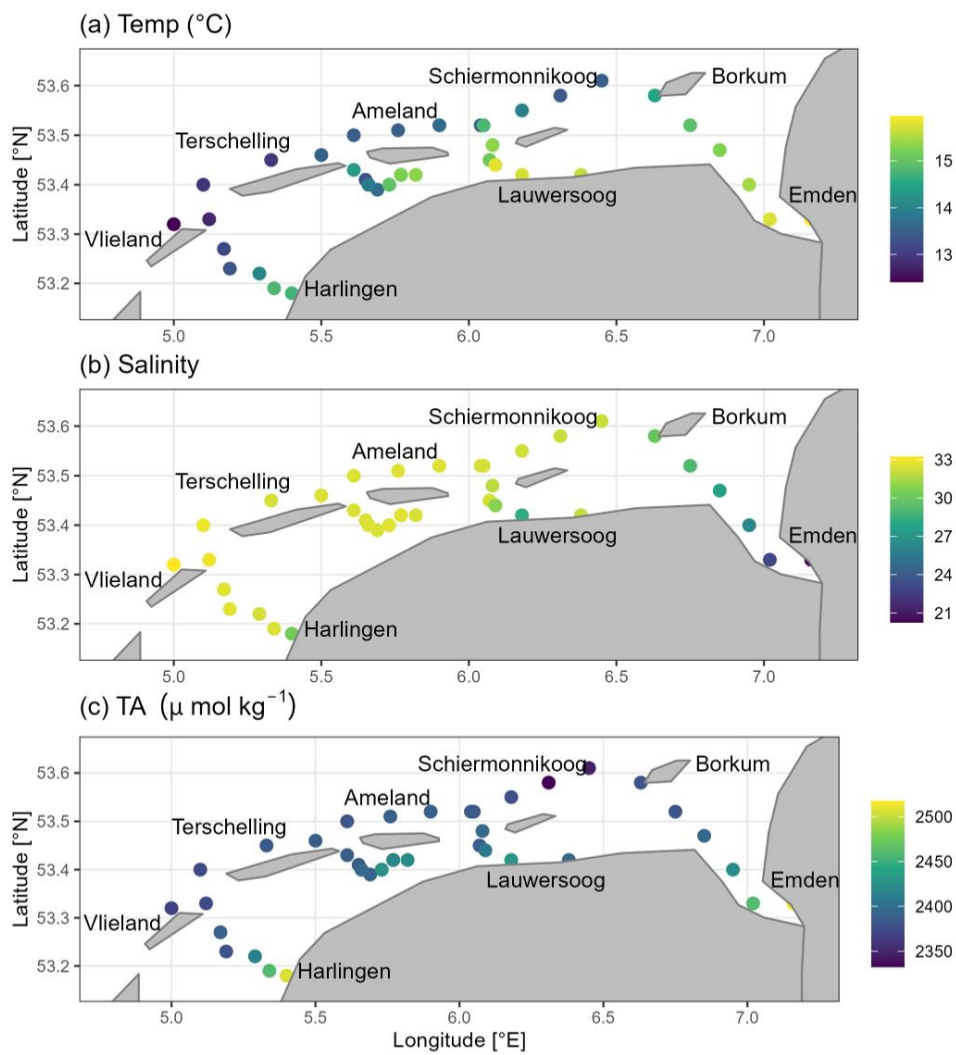
Figure 2 Spatial distribution of a) temperature (°C), b) salinity (PSU), and c) total alkalinity (TA; μmol kg⁻¹) from surface water samples in May 2019.

158   Compared to the other transects of this study region, the strong influence of the inner Ems Estuary is visible at the most

159   upstream station in the Ems-Dollard Inlet, showing lowest salinity, lowest pH and calcite saturation state values, and highest

160   values of TA, DIC, nitrate, silicate and phosphate. The outer side of the Vlie Inlet reflects the North Sea conditions with lower

161   temperatures and higher salinities. The North Sea impact is also visible in the mixing plot between TA and salinity (Fig.

162   3).Statistical significant linear mixing behavior was observed in the transect through the Ems-Dollard Inlet (R^2 = 0.81) and

163   through the Vlie Inlet (R^2 = 0.77), where TA concentrations decreased with increasing salinities from the mainland towards

164   the North Sea (Fig. 3). Whereas in the Ems-Dollard Inlet mixing is dominated by riverine water with high TA concentrations,

165   the mixing in the Vlie Inlet showed a more prominent mixing of Wadden Sea and North Sea water. The TA concentrations in

166   the Vlie Inlet and around Ameland, both at the North Sea side (Ameland NS) and the Wadden Sea side (Ameland WS) were

167   higher than the TA concentration computed for the salinity end-member in the Ems-Dollard Inlet, suggesting the Dutch

168   Wadden Sea as a source of TA (Fig. 3). Both the Ameland NS and WS data clearly indicated a non-conservative behavior with

169   a range of TA concentrations at near constant salinities.
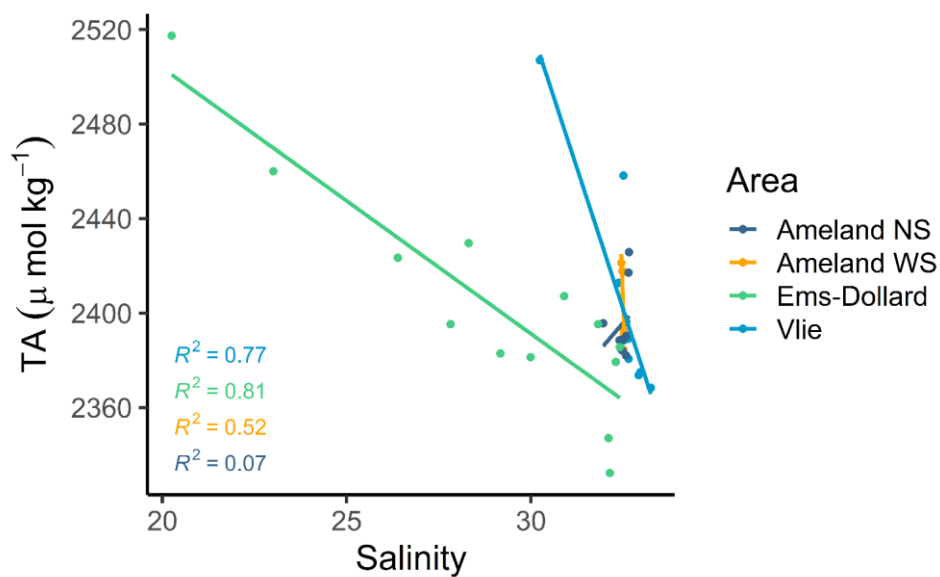
170

171 **Figure 3** Mixing plot of total alkalinity (TA) and salinity (PSU) in the North Sea side of Ameland and the Frisian Inlet

172 (Ameland NS), in the Wadden Sea site of Ameland (Ameland WS), around Schiermonnikoog and in the Ems-Dollard Inlet

173 (Ems-Dollard), and in the Vlie Inlet (Vlie).

174 **3.2 Tidal cycle**

175 We observed a half tidal cycle at an anchor station in the Ameland Inlet during ebb tide, to 1) identify potential TA sources

176 and 2) to quantify potential TA export to the North Sea. We identified patterns in several biogeochemical parameters in water

177 leaving the tidal flats (Fig. 4, Table B1). Temperature increased from 13.25 to 14.7 °C (Fig. 4a). Salinity was constant around

178 32.5 (Fig. 4b, Table B1), which is in the range of coastal southern North Sea water excluding admixture of local fresh water

179 sources.

180 During ebb tide, TA ranged from 2387 µmol TA kg^{-1} during high tide to 2438 µmol TA kg^{-1} during low tide (Fig. 4c). We

181 observed an increase of 51.6 µmol TA kg^{-1} (ΔTA) during ebb tide (6.8 h), resulting in a TA increase of 7.6 µmol TA kg^{-1} h^{-1}

182 at the sampling location.

183 DIC concentrations behaved similar to TA with minimum values at high tide (2172 µmol DIC kg^{-1}), and maximum values

184 (2273 µmol DIC kg^{-1}) at low tide, resulting in an increase of 101.3 µmol DIC kg^{-1} (ΔDIC) or 14.9 µmol DIC kg^{-1} h^{-1} (Fig. 4d).

185 DIC increased almost twice as much as TA.

186 Nitrate increased during ebb tide by 0.92 µmol NO$_3^-$ L^{-1} (ΔNO$_3^-$) from a minimum of 1.26 µmol NO$_3^-$ L^{-1} to a maximum of

187 2.17 µmol NO$_3^-$ L^{-1} (Fig. 4e), resulting in a nitrate increase of 0.13 µmol NO$_3^-$ L^{-1} h^{-1}.

188 Silicate showed a similar pattern with low values (1.8 µmol Si L^{-1}) at high tide increasing during ebb tide to a maximum of

189 11.2 µmol Si L^{-1}, resulting in a silicate increase (ΔSi) of 9.4 µmol Si L^{-1} or 1.4 µmol Si L^{-1} h^{-1} during ebb tide (Fig. 4f).

190 Ammonium increased from 3.47 µmol NH$_4^+$ L^{-1} to 6.22 µmol NH$_4^+$ L^{-1} during ebb tide (Fig. 4g), resulting in an ammonium

191 increase (ΔNH$_4^+$) of 2.74 µmol NH$_4^+$ L^{-1}, or 0.4 µmol NH$_4^+$ L^{-1} h^{-1}.

192 The calcite and aragonite saturation states had maximum values (Ω_{Ca} = 3.8, Ω_{Ar} = 2.4) at high tide and decreased to their

193 minimum (Ω_{Ca} = 3.1, Ω_{Ar} = 2.0) during ebb tide (Fig. 4h,i). The influence of the North Sea is indicated by the observed

194 maximum at high tide, which decreased during the ebb.

195 The seawater pCO$_2$ had minimum values at high tide (385.1 µatm) and increased up to 576.6 µatm during low tide (Fig. 4i).

196 Like Ω omega, the maximum pH was 8.07 at high tide and decreased to a minimum (7.93) during ebb tide (Fig. 4j).

197 C$_{org}$:N ratios of SPM increased during ebb tide (Fig. 4k). A minimum C$_{org}$:N ratio of 5.6 was observed around high tide and

198 increased to a maximum of 13.0 during ebb tide. Simultaneously, the SPM concentration increased during ebb tide, from 12.8

199 mg SPM L^{-1} to a maximum of 82.4 mg SPM L^{-1} at the second last station (Table B1).

202
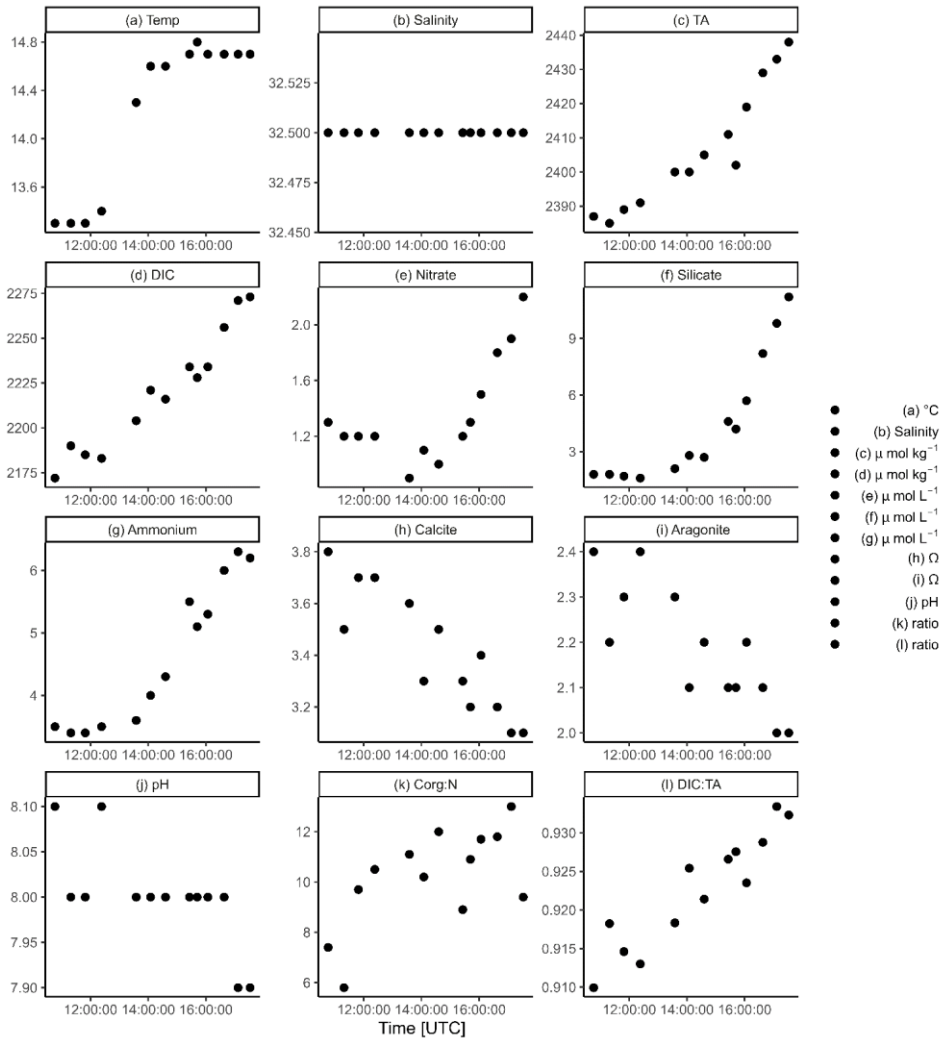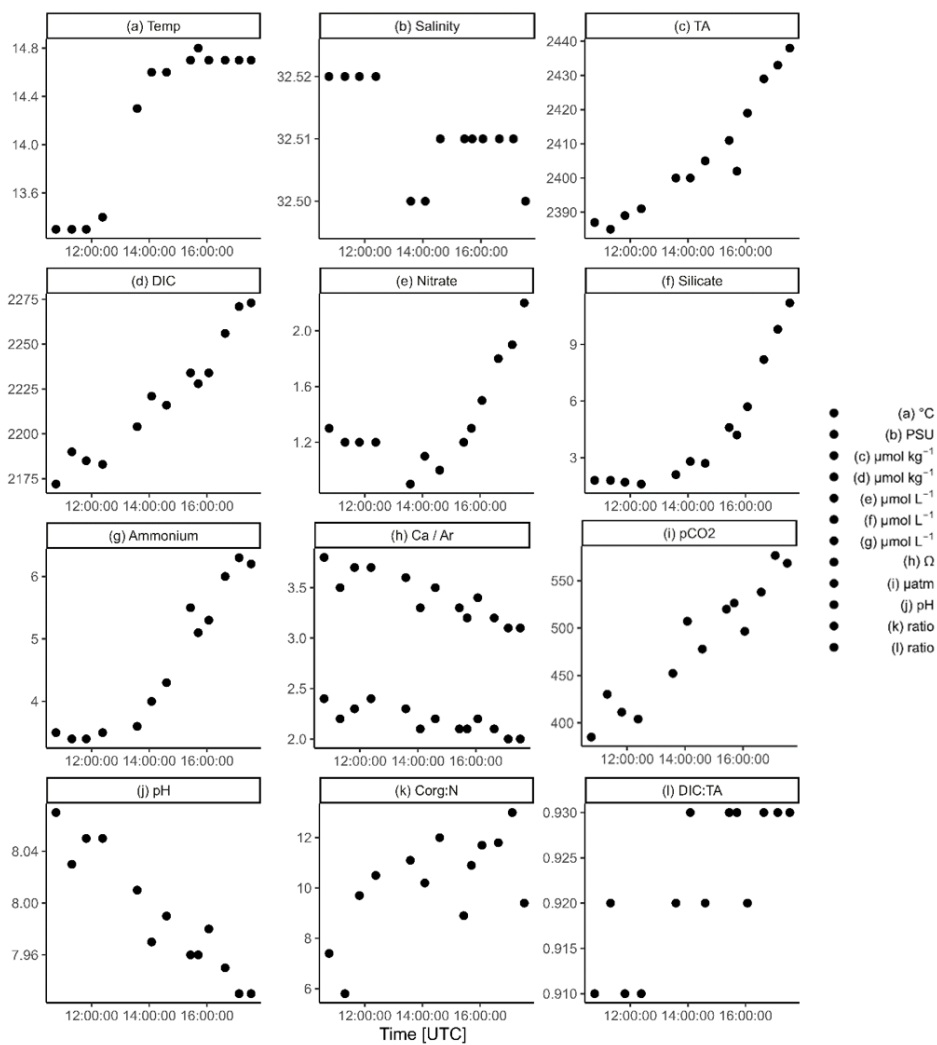
Figure 4 A half tidal cycle from high tide to low tide. Temporal distribution of a) temperature, b) salinity, c) total alkalinity
(TA), d) dissolved inorganic carbon (DIC), e) nitrate, f) silicate, g) ammonium, h) calcite (upper points) and aragonite (lower

205 points) saturation states (Ω), i) pCO$_2$ (μatm), j) pH, k) C$_{org}$:N ratio of SPM, and l) DIC:TA ratio. Note the different y-axes

206 and the +1 hour time difference between the local time and the UTC time.

3.3 TA generation

208 Tidal forcing leads to a bi-diurnal exchange between Wadden Sea and North Sea water. The tidal forcing also induces a strong

209 benthic-pelagic coupling (Huettel et al., 2003;Røy et al., 2008). Many studies support that the outflowing water exports

210 material from the sediment including remineralization products from organic matter (e.g., Billerbeck et al., 2006;Røy et al.,

211 2008). Here, we focus on the hypothesis that the sediments are a significant source of TA.

212 For a first rough estimate of a maximum TA export during ebb tide, we used the mean observed TA increase (ΔTA / 2) of 25.8

213 μmol TA kg^{-1} during ebb tide (in the Ameland Inlet, part of the Borndiep tidal basin), a tidal prism of 478 *10^6 m^3 of the

214 Borndiep tidal basin, and a share of intertidal flats of 53 % (Louters and Gerritsen, 1994). Assuming that only the intertidal

215 sediments exchange TA, we estimated a TA export of 6.6 Mmol TA per tide to the North Sea. Assuming two ebb tides and a

216 lunar cycle of 24.8 hours this would result in a daily export of 12.7 Mmol TA.

217 The significant correlation of TA and silicate (R^2 = 0.93), and the insignificant relation between TA and salinity (R^2 = 0.32),

218 as well as silicate and salinity (R^2 = 0.21), suggest that TA originates from the tidal flats in this part of the Dutch Wadden Sea

219 and is not from admixture carried by river runoff. The significant correlation between TA and silicate both during ebb tide

220 point to the same source (Fig. 5b).

221 To further elucidate potential TA sources in the Dutch Wadden Sea, we correlated TA with DIC, silicate, nitrate, and

222 ammonium in the half tidal cycle from high tide to low tide, respectively (Fig. 5).

223 The correlation between TA and DIC is a measure between anaerobic and aerobic processes. Our data show a strong positive

224 correlation between DIC and TA (R^2 = 0.93) with TA concentrations being higher than DIC concentrations (Fig. 5a). We

225 observed a release excess of DIC compared to TA as indicated by the slope of 1.89 and by an increase in DIC (ΔDIC = 101.3

226 μmol kg^{-1}) almost twice as high as TA (ΔTA = 51.6 μmol kg^{-1}) (Fig. 5a). This excess DIC may be caused by strong CO$_2$

227 production due to high aerobic OM degradation, which can be supported by seawater being supersaturated in pCO$_2$ with respect

228 to the atmosphere (Fig. 4i, Table B1). or by uptake from the atmosphere due to water movement by tidal forcing. However,

229 given the heterotrophic nature of the Wadden Sea (e.g., van Beusekom et al., 2012), a CO$_2$ undersaturation is unlikely. The

230 TA increase can be fueled by various processes which we will discuss below. We detected a linear positive correlation of

231 increasing TA and silicate (R^2 = 0.93) during ebb tide, supporting pore water outflow (Fig. 5b) as pore water is the major Si

232 source during summer (van Bennekom et al., 1974). A stronger influence of the pore water with ongoing ebb tide is indicated

233 by increasing values. The positive correlation between nitrate and TA (R^2 = 0.67) (Fig. 5c) was less strong than the correlations

234 between TA and DIC, and TA and Si, which could be traced back to on an effect of the first four samplings points that were

235 probably at the tipping point from high tide to low tide. In the remaining samples, the increasing nitrate and TA concentrations

236 suggest a stronger TA generation than nitrate production, balancing TA that may be consumed by nitrification (i.e., nitrate

237 production).

238
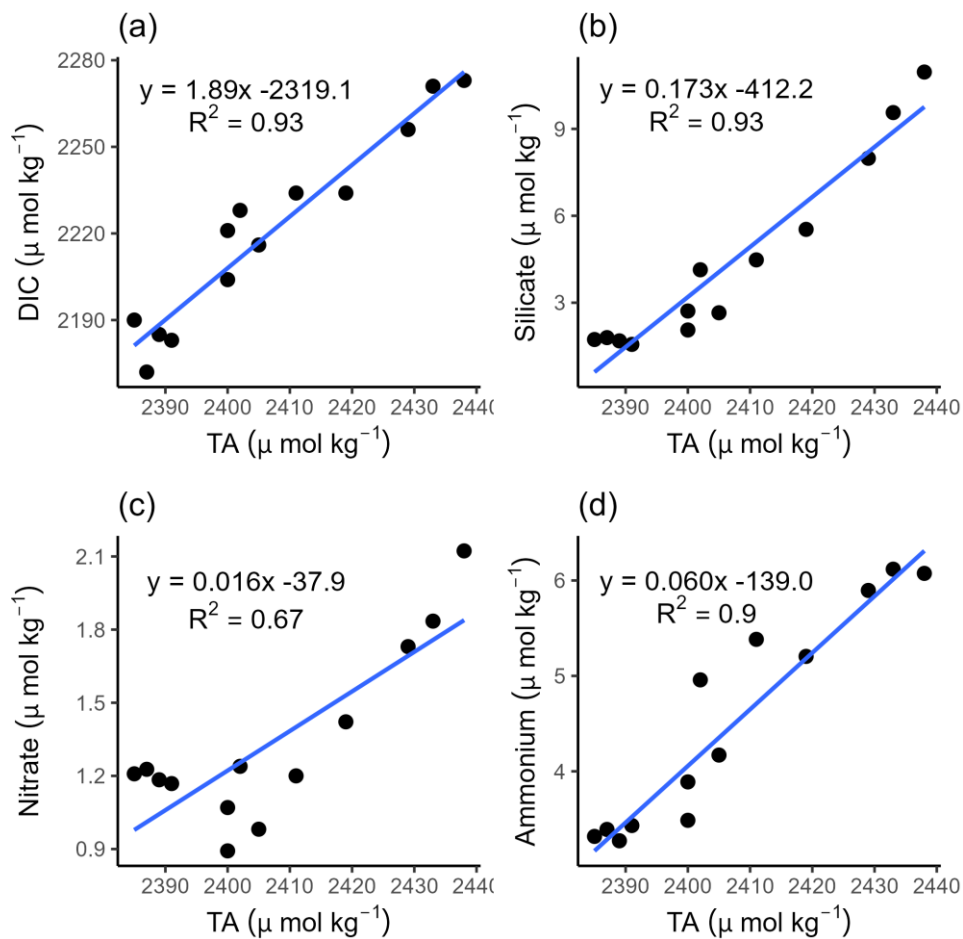
Figure 5 Correlations of TA with a) dissolved inorganic carbon (DIC), b) silicate, c) nitrate, and d) ammonium during ebb
tide in the Ameland Inlet.

4 Discussion

4.1 Spatial TA variability

Hoppema (1990) reported TA distributions in the westernmost part of the Dutch Wadden Sea around the barrier islands Texel, Vlieland, and Terschelling. He focused on the tidal basins drained by the tidal inlets Marsdiep and Vlie located more to the west than our sampling stations (not visible on the map). Hoppema (1990) did not observe a continuous increase of salinity in the Wadden Sea from the fresh water source towards the North Sea and associated this to the influence of tidal differences and an arbitrary sampling scheme. The presence (dominance) of North Sea water in the Dutch Wadden Sea and on the tidal flats is supported by our transect data, which show relatively high salinities at coastal North Sea level. Brackish salinities were only detected in the ~~large~~ Ems-Dollard Inlet, which receives fresh water from the river Ems, and close to Harlingen and Lauwersoog, which have direct fresh water inflows by smaller rivers and streams. The absence of clear salinity gradients in the more eastern part of the Dutch Wadden Sea investigated in our study suggest that most of the IJsselmeer discharge was exchanged with the North Sea through the Marsdiep (e.g., Duran-Matute et al., 2014).

The spatial TA data by Hoppema (1990), show lower TA concentrations at stations with more fresh water influence and higher TA concentrations in the tidal inlets. The data of this study also show high TA concentrations in the tidal inlets, suggesting TA generation in sediments, which is possibly fueled by high imports of nutrients and OM (van Beusekom and De Jonge, 2002). The even higher TA concentrations at stations with lower salinities close to the mainland observed in this study also show the influence from the catchment area on the coast, and possibly TA generation in the shallow sediments near the coast. In May ~~(1986)~~, Hoppema (1990) found TA concentrations ranging between 2319 and 2444 µmol TA kg^{-1} at salinities between 18.62 and 29.17. Our lowest observed TA concentration was 2332 µmol TA kg^{-1} at a salinity of 32.14, and our highest TA concentration was 2517 µmol TA kg^{-1} at a salinity of 20.25 close to the coastal mainland. A comparison of both studies shows that the general TA levels are in a similar range, but that the spatial gradients are opposite.

A conservative mixing between TA and salinity is only visible in the Ems-Dollard Inlet and the Vlie Inlet (Fig. 3). While the conservative mixing in the Ems-Dollard Inlet is more dominated by the fresh water discharge from the Ems River, the conservative mixing in the Vlie Inlet is more dominated by North Sea water passing through this deep inlet and allowing more North Sea water to be transported towards the coast. After the Marsdiep Inlet, the Vlie Inlet has the highest average tidal prism and is the second largest inlet in the Dutch Wadden Sea (Elias et al., 2012). Similar to our findings, Hoppema (1990) noted a linear mixing of TA and salinity in the Vlie Inlet, and suspected a lower fresh water contribution there as well, which is in accordance with model data (Duran-Matute et al., 2014).

In the Ems-Dollard Inlet, conservative mixing was observed, indicating minor contributions from other sources. In a previous study, Norbisrath et al. (2023) observed very high TA concentrations and TA generation in the upper tidal river of the highly turbid Ems Estuary, which may explain the high levels of TA in the Ems-Dollard Inlet (at low salinities) observed in this study.

273 Hoppema (1990) also observed a range of TA concentrations in the Dutch Wadden Sea and related these to different sinks and
274 sources. TA sinks can be calcium carbonate ($CaCO_3$) precipitation, or extraction of seawater carbonate by mollusks (e.g., Chen
275 and Wang, 1999;Hoppema, 1990). Variable fresh water inflows can either serve as a sink or a source (e.g., Chen and Wang,
276 1999;Hoppema, 1990). Other TA sources can be $CaCO_3$ dissolution, anaerobic metabolic processes in the sediment, or erosion
277 of TA enhancing sediments (e.g., Hoppema, 1990;Chen and Wang, 1999).
278 Except for the Ems-Dollard Inlet and close to Harlingen, we observed mainly marine salinities (> 30) but higher TA values in
279 the Dutch Wadden Sea than in the North Sea. We therefore exclude possible TA sinks and focus only on TA sources. According
280 to Hoppema (1990), the main causes for TA variations in the Dutch Wadden Sea were fresh water inflows and sources in the
281 sediment. In our study, fresh water inflows with high TA concentrations were only observed in the Ems-Dollard Inlet, but not
282 around the islands and the tidal flats. For a further TA source identification in the Dutch Wadden Sea, we investigated the TA
283 variability during ebb tide in a tidal channel close to Ameland.

284 4.2 Determination of TA generation

285 Burt et al. (2016) and Schwichtenberg et al. (2020) indicated TA generation in the Wadden Sea as an important source for the
286 North Sea's carbon storage capacity. Here, we want to further identify TA generation and potential TA sources.
287 In a study from the late 1980s, Hoppema (1993) observed a tidal cycle in the Marsdiep in May and September. Focusing on
288 TA, DIC, and oxygen, he also observed increasing TA values during ebb tide and assumed the tidal flats and discharging rivers
289 and canals as TA sources. Comparing our present TA data and the historical TA data, there is not a large difference in the
290 range of values observed during a tidal cycle. However, a further in-depth interpretation and comparison of both TA data sets
291 is limited by the low number of data, leading us to focus on TA generation during our cruise.
292 We made a very rough first estimate of the daily TA export. By using a 3D ecosystem model, Schwichtenberg et al. (2020)
293 estimated an annual export of 10 to 14 Gmol TA yr^{-1} for the entire Dutch Wadden Sea. Given that the Borndiep tidal basin
294 covers about 14% of the Dutch Wadden Sea and assuming no seasonal dynamics, our estimate of 12.7 Mmol d^{-1} compares
295 well with the annual averaged model estimate of 4.6 Mmol TA d^{-1}, but the overestimation suggests that seasonal dynamics
296 may be involved. Since our TA export based only on a half tidal observation, the inclusion of it into the model used by
297 Schwichtenberg et al. (2020) would be unreliable (pers. comm. J. Pätsch, 2022). To test whether the observed TA generation
298 matches their suggested TA export, observational data of at least each season are required to run the model and gain a
299 representative result (pers. comm. J. Pätsch, 2022).

300 4.3 TA source attribution

301 4.3.1 Local sediment outwash

302 In order to gain further insight into potential sources of TA, we compared our TA and nutrient data. The main focus was on
303 dissolved silicate (Si) as van Bennekom et al. (1974) showed that this nutrient is depleted in the Wadden Sea during the spring

304 diatom blooms and further showed that pore water is the main source of dissolved Si during summer. It is important to note
305 that winter concentrations in the Rhine (main contributor to the IJsselmeer) have not changed much since the 1970s and
306 showing maximum concentrations of about 125 µmol Si L^{-1} in winter and clear seasonal dynamics due to uptake by diatoms
307 (unpublished results based on data provided by Pätsch (2024); available through https://wiki.cen.uni-
308 hamburg.de/ifm/ECOHAM/DATA_RIVER). We identified a silicate increase of 1.4 µmol Si L^{-1} h^{-1} during ebb tide. Due to
309 the absence of large estuaries nearby and salinity consistently being above 32 at our tidal sampling station near around the
310 island of Ameland, we exclude fresh water runoff as a major silicate source and indicate TA sources within the Wadden Sea.
311 Submarine groundwater discharge (SGD) was identified as a source for nutrient fluxes in tidal flat ecosystems in previous
312 studies (e.g., Billerbeck et al., 2006;Røy et al., 2008;Santos et al., 2021;Waska and Kim, 2011;Wu et al., 2013). Since we
313 observed relatively constant marine salinities, we suspect that deep pore water flow (e.g., Røy et al., 2008) enriched with
314 nutrients act as a source for our observed increasing TA and nutrients parameters. TA generation in tidal flats was also observed
315 by Faber et al. (2014), who focused on a large macro tidal embayment in southern Australia. They also found increasing TA
316 values during ebb tide, associated the TA increase with a higher fraction of pore water, and determined the tidal cycle as the
317 controlling force for pore water exchange. Their findings and the observed silicate outwash support our assumption that TA is
318 generated in the sediments of the tidal flats and is washed out during ebb tide. In addition, we exclude lateral advected signals
319 from more western regions as the Vlie Inlet, since the TA concentrations in the surface transect samples in the Vlie Inlet
320 (except of the two samples close to the coastal mainland near Harlingen) were in the same range as the other observed TA
321 concentrations and were smaller than the increasing TA concentrations during ebb tide. Both increases in TA and silicate are
322 tidal signals, and we identify TA generation in the sediments of the tidal flats here as the major local TA source.

323 **4.3.2 TA generating processes**

324 The deduced observed TA generation of 7.6 µmol TA kg^{-1} h^{-1} and the silicate increase of 1.4 µmol Si L^{-1} h^{-1} indicated an
325 excess of TA compared to silicate (also Fig. 5b). Considering a supposed A given TA:Si ratio of 2:1 (Marx et al. 2017), the
326 observed 1.4 µmol Si L^{-1} h^{-1} would then account for a TA generation of 2.8 µmol TA kg^{-1} h^{-1}. High Si concentrations in tidal
327 flat pore water (Rutgers van der Loeff, 1974) and in situ production of Si from dissolving diatom frustules are the most probable
328 sources of the Si (e.g., van Bennekom et al., 1974). Since we observed more TA generated than silicate being washed out,
329 other biogeochemical processes must be responsible for the TA generation in the sediments of the tidal flats in the Dutch
330 Wadden Sea.
331
332 We exclude $CaCO_3$ dissolution as TA source in the overlying water column, since the Ω values were clearly supersaturated
333 with Ω > 1 (Fig. 4h,i, Table B1). The continuous calcite supersaturation nicely indicated the inflow and dominance of North
334 Sea water during the flood, with Ω values similar to previously observed North Sea values (Ω ~ 3.5 to 4) (Charalampopoulou
335 et al., 2011;Carter et al., 2014). In pore water, carbonate undersaturation and associated $CaCO_3$ dissolution can only be driven

336 metabolically, due to CO_2 production by OM remineralization, or due to the reoxidation of compounds reduced previously by
337 anaerobic processes (Brenner et al., 2016;Jahnke et al., 1994).
338

339 Other potential sources of TA generation in the sediments can be further narrowed down by a more detailed interpretation of
340 changes both in DIC (ΔDIC) and TA (ΔTA) during ebb tide, and their combination with various nutrient ratios. The correlation
341 of DIC and TA reveals an increase in DIC (ΔDIC) almost twice as high as in TA (ΔTA) excess of released DIC compared to
342 TA (Fig. 5a), as indicated by the slope of 1.89.7, while we observed an increase in DIC (ΔDIC) almost twice as high as in TA
343 (ΔTA). The high ΔDIC points to high aerobic OM degradation and remineralization, resulting in high CO_2 production, which
344 is also indicated by seawater being supersaturated in $p$$CO_2$. High aerobic OM degradation was also previously observed in the
345 heterotrophic Wadden Sea (e.g., De Beer et al., 2005;van Beusekom et al., 1999), assuming an OM degradation and
346 remineralization occurring in the water and sediment in about equal parts (van Beusekom et al., 1999). High OM degradation
347 is indicated by the increasing C_{org}:N ratios of SPM during ebb tide (Fig. 4k, Table B1). Because we observed constant coastal
348 North Sea salinities, we rule out fresh water runoff and terrestrial signals as source for the increasing C_{org}:N ratios of SPM.
349 We assume that fresh OM is rapidly degraded in the water column, and the older OM settles on and in the sediment where the
350 degradation continues and where it is resuspended at the low prevailing water levels during ebb. Therefore, we assume that
351 the increase of SPM concentrations and their C_{org}:N ratios is an indicator for older and more refractory OM. The increase in
352 TA concentrations point to anaerobic processes, $CaCO_3$ dissolution, or a combination thereof as TA sources occurring in the
353 sediments.
354

355 For an upper bound estimate of sedimentary $CaCO_3$ dissolution as source of TA, we considered a ΔDIC: ΔTA ratio of 1:2.
356 Considering this ratio and the observed ΔTA of 51.6 µmol TA kg^{-1}, $CaCO_3$ dissolution would lead to a potential ΔDIC of 25.8
357 µmol DIC kg^{-1}. The remaining potential 75.5 µmol DIC kg^{-1} (101.3 – 25.8 µmol DIC kg^{-1}) of the observed (ΔDIC in this study)
358 could then be produced by OM degradation and remineralization, and would, using the theoretical expected Redfield ratio of
359 C:N (6.6) for fresh OM (Hickel, 1984), correspond to an estimated potential dissolved inorganic nitrogen (DIN) production of
360 11.4 µmol DIN kg^{-1}. However, this estimated potential DIN production (11.4 µmol DIN kg^{-1}) of OM degradation and
361 remineralization exceeds the observed increase of ΔDIN (3.97 µmol DIN L^{-1}; Table B1, sum of NO_3^-, NO_2^- and NH_4^+) during
362 ebb tide. Based on this estimation and the assumption that all DIN produced is released and thus lost, TA is probably produced
363 by $CaCO_3$ dissolution and anaerobic metabolic processes other than denitrification in the sediment. In addition to that, and
364 with an N-focused perspective, the DIN loss also hints to the occurrence of other processes that consume nitrogen species but
365 have no net effect on TA, such as anammox and coupled nitrification-denitrification (Hu and Cai, 2011;Middelburg et al.,
366 2020). The suggested DIN loss can be supported by considering the marine DIN:Si ratio, which is supposed to be about 1:1
367 (Brzezinski, 1985). We observed DIN:Si ratios decreasing from 2.7 to 0.8 during ebb tide, showing that both parameter
368 concentrations increased, whereby DIN concentrations increased less than silicate concentrations. The silicate excess with
369 respect to DIN at the end of ebb tide supports the DIN loss.

370 Denitrification, the anaerobic irreversible reduction of NO_3^- to N_2 that generates 0.9 mole TA by using 1 mole NO_3^- as electron

371 acceptor (Chen and Wang, 1999) is a net TA source. Denitrification depends on the supply of nitrate, which seasonally varies

372 (van der Zee and Chou, 2005 and references therein). Generally, nitrate is depleted in summer due to high photosynthetic

373 activity and occurs in higher concentrations in winter (Kieskamp et al., 1991;Jensen et al., 1996;van der Zee and Chou, 2005).

374 This seasonality leads to denitrification rates also being lower in summer and higher in winter (Kieskamp et al., 1991;Jensen

375 et al., 1996). In previous studies, Faber et al. (2014) identified denitrification as a minor source of TA due to low denitrification

376 rates, and also Kieskamp et al. (1991) observed low denitrification rates in the Wadden Sea, with low nitrate concentrations

377 (< 2.5 µmol L^{-1}) in the ~~overlying~~ water column. We observed nitrate concentrations (< 2.17 µmol L^{-1}) lower than the

378 concentration sufficient for denitrification assumed by Kieskamp et al. (1991). Therefore, we do not exclude denitrification,

379 but suspect it as a minor source of TA in the Dutch Wadden Sea at least in spring and summer due to the seasonal lack of

380 nitrate. Thomas et al. (2009) detected TA seasonality in the southern bight of the North Sea, which is also influenced by the

381 TA generation in the Wadden Sea. ~~We support their findings of lowered TA generation by denitrification in late spring and~~

382 ~~early summer.~~ In addition, the ~~calculated~~ estimated potential DIN production ~~excess~~ compared to the observed DIN not only

383 hints to other N consuming processes that have no effect on TA, but also suggests that allochthonous nitrate would be needed

384 to fuel the TA increase by denitrification. ~~In addition, the albeit low availability of nitrate indicates to predominantly aerobic~~

385 ~~metabolic activity in the overlying water and upper sediment layers during the time of our observations, which is in line with~~

386 ~~earlier studies reporting an enhanced relevance of anaerobic activity later in summer (Luff and Moll, 2004;Thomas et al.,~~

387 ~~2009).~~

388

389 The simultaneous increase of ammonium and TA (Fig. 4c, 4d, 5d) is important to notice, because under oxic conditions the

390 occurrence of ammonium is coupled with nitrification, a process that consumes ammonium and also TA (Chen and Wang,

391 1999). However, under anoxic conditions, such as in deeper sediment layers, ammonium cannot be reoxidized, accumulates,

392 and is washed out during ebb tide. Since we observed low nitrate concentrations and rule out terrestrial nitrate inputs here, the

393 increase in ammonium and TA implies the occurrence of other anaerobic processes of the redox system, such as sulfate and

394 iron reduction, to generate TA in the deeper, anoxic sediment layers in the Dutch Wadden Sea.

395 Sulfate reduction followed by iron reduction and the formation and burial of pyrite are net sources of TA, since TA

396 consumption by reoxidation is excluded when buried in sediments (Berner et al., 1970;Faber et al., 2014). Whether and to what

397 extent these processes contribute to TA generation in the deeper sediments of the Dutch Wadden Sea cannot be further

398 identified without the necessary data. However, sulfate reduction was also mentioned as source of TA by Thomas et al. (2009).

399 And t~~T~~he temporary slight appearance of noticeable sulfuric odor could be another indirect indicator for the occurrence of

400 sulfate reduction. In previous studies of tidal flats in the German Wadden Sea, Beck et al. (2008a);(2008b) observed increasing

401 TA concentrations with depth and identified sulfate reduction as the most important process for anaerobic OM remineralization

402 in pore water cores.

403

404 A strict comparison of the more northern (north of the Elbe Estuary) and the more western (Texel – Elbe Estuary) parts of the
405 Wadden Sea is difficult because the areas vary in terms of OM import and eutrophication effects (van Beusekom et al., 2019),
406 sediment composition, and extent between the barrier islands and the mainland, all of which influence the occurrence and
407 interaction of biogeochemical processes (Schwichtenberg et al., 2020). The area characteristics of the northern and western
408 Wadden Sea differ especially in terms of OM turnover being lower in the norther Wadden Sea. A previous study by Brasse et
409 al. (1999) identified high TA and DIC concentrations in the sediment of the North Frisian Wadden Sea and identified $CaCO_3$
410 dissolution and sulfate reduction as major TA sources, which is consistent with our findings.

5 Conclusion

412 The Dutch Wadden Sea is a unique and highly dynamic ecosystem. We observed higher TA values in the Dutch Wadden Sea
413 than in the North Sea and identified the Dutch Wadden Sea as a TA source for the North Sea's carbonate system. Compared
414 to previous studies (Hoppema, 1990, 1993), the TA values we observed were in a similar range, with high TA values in the
415 tidal basins. Beside the need for seasonal observations, future work should also focus on regional and seasonal impacts of fresh
416 water inflows of TA on the TA status in the Dutch Wadden Sea.
417 By observing salinity and using dissolved silicate as a tracer, we excluded fresh water and river runoff as significant TA sources
418 on the tidal flats, and instead, deduced local outwash from the sediments as sources of TA. Considering various stoichiometries,
419 we suggest that $CaCO_3$ dissolution generates TA in the more upper oxic sediment layers, and anaerobic, metabolic processes
420 such as denitrification, sulfate and iron reduction are potential TA sources in the deeper anoxic sediment layers. However, in
421 spring and early summer, denitrification seems to play a minor role in generating TA in the sediments of the Dutch Wadden
422 Sea due to seasonality and associated limited nitrate availability.

423 **6 Appendices**

424 **Appendix A**

425
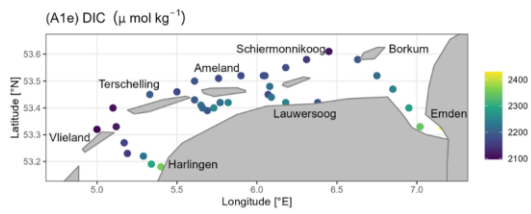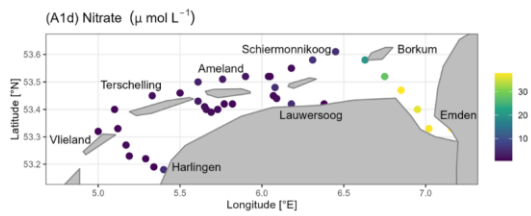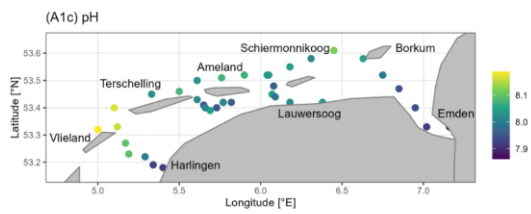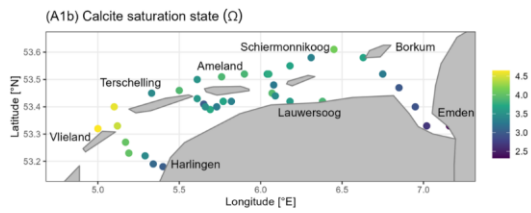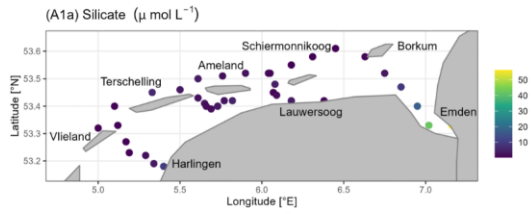
426 **Figure A1** Spatial distribution of A1a) silicate (Si; µmol L^{-1}), A1b) calcite saturation state (Ω), A1c) pH, A1d) nitrate (NO_3^-;

427 µmol L^{-1}), and A1e) dissolved inorganic carbon (DIC; µmol kg^{-1}) from surface water samples in May 2019.

428

Appendix B

Table B1 Half tidal cycle sample parameter during ebb tide. Sample no. 545 is the first sample at high tide and sample no. 557 is the last sample at low tide on 21 May 2019 (53.38°N & 5.62°E). Shown are ~~rounded up~~ values of temperature (Temp), salinity (Sal), total alkalinity (TA), dissolved inorganic carbon (DIC), silicate (Si), nitrate (NO_3^-), nitrite (NO_2^-), ammonium (NH_4^+), phosphate (PO_4^{3-}), dissolved inorganic nitrogen (DIN), the amount of carbon (C) and organic carbon (C_{org}) of SPM, the amount of nitrogen (N) of SPM, the calcite (Ca) and aragonite (Ar) saturation states, the pH, and the seawater partial pressure of CO_2 (pCO_2) per sample.

Sample No.	Time [UTC]	Temp [°C]	Sal [PSU]	TA / DIC [µmol kg^{-1}]	Si [µmol L^{-1}]	NO_3^- [µmol L^{-1}]	NO_2^- [µmol L^{-1}]	NH_4^+ [µmol L^{-1}]	PO_4^{3-} [µmol L^{-1}]
545	10:46	13.26	32.52	2387 / 2172	1.84	1.26	0.19	3.47	0.12
546	11:19	13.25	32.52	2385 / 2190	1.77	1.24	0.19	3.40	0.11
547	11:49	13.28	32.52	2389 / 2185	1.72	1.21	0.19	3.35	0.11
548	12:23	13.38	32.52	2391 / 2183	1.6	1.19	0.19	3.52	0.12
549	13:35	14.32	32.50	2400 / 2204	2.11	0.91	0.25	3.57	0.32
550	14:05	14.61	32.50	2400 / 2221	2.78	1.09	0.29	3.98	0.42
551	14:36	14.64	32.51	2405 / 2216	2.72	1.01	0.29	4.27	0.47
552	15:26	14.73	32.51	2411 / 2234	4.59	1.23	0.34	5.51	0.57
553	15:42	14.77	32.51	2402 / 2228	4.24	1.26	0.33	5.08	0.54
554	16:04	14.72	32.51	2419 / 2234	5.66	1.46	0.36	5.33	0.54
555	16:38	14.66	32.51	2428 / 2256	8.18	1.77	0.43	6.04	0.58
556	17:07	14.68	32.51	2433 / 2271	9.79	1.87	0.47	6.27	0.62
557	17:32	14.70	32.50	2438 / 2273	11.22	2.17	0.50	6.22	0.63

Sample No.	Time [UTC]	DIN [µmol L^{-1}]	C / C_{org} (SPM) [µmol L^{-1}]	N (SPM) [µmol L^{-1}]	C_{org}:N (SPM)	SPM [mg L^{-1}]	Ca / Ar [Ω]	pH	pCO_2 [µatm]
545	10:46	4.93	86.8 / 65.1	8.8	7.4	12.8	3.8 / 2.4	8.07	385.1
546	11:19	4.83	72.7 / 42.4	7.4	5.8	8.7	3.5 / 2.3	8.03	430.2
547	11:49	4.76	112.4 / 93.4	9.6	9.7	15.4	3.7 / 2.3	8.05	411.4
548	12:23	4.91	108.5 / 104.6	9.9	10.5	16.8	3.7 / 2.4	8.05	404.1
549	13:35	4.73	111.1 / 97.8	8.8	11.1	13.9	3.6 / 2.3	8.01	452.3
550	14:05	5.37	233.0 / 180.3	17.7	10.2	32.2	3.3 / 2.1	7.97	507.2
551	14:36	5.56	193.2 / 174.3	14.5	12.0	29.6	3.5 / 2.2	7.99	477.9
552	15:26	7.08	248.6 / 163.5	18.4	8.9	34.3	3.3 / 2.1	7.96	520.0
553	15:42	6.67	257.6 / 199.3	18.3	10.9	41.6	3.2 / 2.1	7.95	526.4
554	16:04	7.15	324.4 / 271.1	23.2	11.7	55.0	3.4 / 2.2	7.98	496.6
555	16:38	8.24	440.4 / 345.2	29.2	11.8	75.7	3.2 / 2.1	7.95	538.0
556	17:07	8.61	430.5 / 363.3	27.9	13.0	82.4	3.1/ 2.0	7.93.	576.6

Sample No.	Time [UTC]	Temp [°C]	TA / DIC [μmol kg⁻¹]	Si [μmol L⁻¹]	NO₃⁻ [μmol L⁻¹]	NO₂⁻ [μmol L⁻¹]	Ca / Ar [Ω]	pH	pCO₂ [μatm]
557	17:32	8.90	308.9 / 199.1	21.2	9.4	48.8	3.1 / 2.0	7.93	568.4

Table B2 Half tidal cycle sample parameter during high tide. Sample no. 564 is the first sample at low tide and sample no. 578 is the last sample at high tide on 23 May 2019 (53.39°N & 5.63°E, 5.62°E*). Shown are ~~rounded up~~ values of temperature (Temp), salinity (Sal), total alkalinity (TA), dissolved inorganic carbon (DIC), silicate (Si), nitrate (NO₃⁻), nitrite (NO₂⁻), ammonium (NH₄⁺), phosphate (PO₄³⁻), dissolved inorganic nitrogen (DIN), the amount of carbon (C) and organic carbon (C$_{org}$) of SPM, the amount of nitrogen (N) of SPM, the calcite (Ca) and aragonite (Ar) saturation states, the pH, and the seawater partial pressure of CO₂ (pCO₂) per sample.

Sample No.	Time [UTC]	Temp [°C]	Sal [PSU]	TA / DIC [μmol kg⁻¹]	Si [μmol L⁻¹]	NO₃⁻ [μmol L⁻¹]	NO₂⁻ [μmol L⁻¹]	NH₄⁺ [μmol L⁻¹]	PO₄³⁻ [μmol L⁻¹]
564	05:09	14.04	32.667	2431 / 2246	8.53	1.25	0.47	3.31	0.38
565	05:32	14.02	32.687	2441 / 2287	9.14	1.26	0.45	3.08	0.37
566	06:01	13.95	32.697	2436 / 2284	8.88	1.33	0.38	2.46	0.34
567	06:33	14.16	32.697	2443 / 2284	8.68	0.95	0.37	2.37	0.33
568	07:02	14.21	32.697	2432 / 2280	6.94	0.75	0.34	2.63	0.32
569	07:31	14.15	32.556	2401 / 2223	2.12	0.98	0.27	4.12	0.33
570	08:04	14.20	32.556	2403 / 2218	2.10	1.04	0.27	3.88	0.30
571	08:35	14.27	32.556	2409 / 2228	2.15	0.92	0.25	4.18	0.32
572	09:04	14.37	32.53	2400 / 2209	1.88	1.00	0.22	3.86	0.26
573	09:34	14.16	32.52	2398 / 2200	1.70	1.03	0.21	3.51	0.21
574*	10:02	14.17	32.52	2391 / 2197	1.72	1.07	0.21	3.40	0.18
575*	10:34	14.11	32.51	2389 / 2195	1.78	1.18	0.20	3.45	0.16
576	11:04	14.21	32.50	2390 / 2187	1.76	1.12	0.19	3.29	0.14
577	11:34	14.50	32.51	2399 / 2193	1.66	1.10	0.20	3.32	0.16
578	12:03	13.96	32.51	2390 / 2187	1.75	1.41	0.19	3.72	0.11

Sample No.	Time [UTC]	DIN [μmol L⁻¹]	C / C$_{org}$ (SPM) [μmol L⁻¹]	N (SPM) [μmol L⁻¹]	C$_{org}$:N (SPM)	SPM [mg L⁻¹]	Ca / Ar [Ω]	pH	pCO₂ [μatm]
564	05:09	5.03	353.7 / 253.2	27.5	9.2	52.3	3.0 / 2.2	7.99	490.3
565	05:32	4.78	333.5 / 220.1	26.1	8.4	49.7	3.0 / 1.9	7.92	592.9
566	06:01	4.17	330.3 / 232.9	25.5	9.1	51.7	2.9 / 1.9	7.91	600.3
567	06:33	3.68	274.7 / 195.7	21.8	9.0	36.9	3.0 / 1.9	7.92	582.6
568	07:02	3.72	317.8 / 220.2	24.5	9.0	46.1	2.9 / 1.9	7.91	601.8
569	07:31	5.37	88.6 / 59.1	7.0	8.5	14.7	3.3 / 2.1	7.98	500.7
570	08:04	5.20	96.8 / 73.6	8.8	8.4	18.1	3.4 / 2.2	7.99	482.6
571	08:35	5.35	114.2 / 109.6	9.9	11.0	14.8	3.3 / 2.1	7.98	497.6

572	09:04	5.08	107.5 / 73.9	9.9	7.5	16.4	3.5 / 2.2	8.00	466.6
573	09:34	4.75	82.1 / 72.7	7.2	10.0	11.8	3.6 / 2.3	8.02	445.3
574*	10:02	4.68	85.2 / 62.9	7.2	8.7	9.9	3.5 / 2.3	8.01	450.5
575*	10:34	4.83	83.5 / 65.9	7.2	9.2	11.1	3.5 / 2.3	8.01	449.6
576	11:04	4.60	82.7 / 52.1	8.2	6.3	8.5	3.7 / 2.3	8.03	429.9
577	11:34	4.62	65.8 / 50.8	6.5	7.8	7.2	3.7 / 2.4	8.03	430.8
578	12:03	5.32	71.6 / 54.6	7.7	7.1	7.7	3.7 / 2.3	8.04	425.3

Table B3 Transect parameter of cruise LP20190515 on RV *Ludwig Prandt* in the Dutch Wadden Sea in May 2019. Shown are values of latitude (Lat), longitude (Lon), temperature (Temp), salinity (Sal), total alkalinity (TA), dissolved inorganic carbon (DIC), silicate (Si), nitrate (NO_3^-), the calcite (Ca) and aragonite (Ar) saturation states, and pH per sample. Our salinity and temperature data were complemented bycompared to data of three Rijkswaterstraat stations, which were close to our stations. There, Dantziggat* (53°24'4.093", 5°43'37.132") showed temperatures of 11.4 and 14.9 °C and salinities of 31.9 and 31.2 on 10 and 27 May 2019, respectively, Terschelling 10** (53°27'37.318", 5°5'58.129") showed temperatures of 11.4 and 12.9 °C and salinities of 32.8 and 33.4 on 15 and 28 May 2019, respectively, and Vliestroom*** (53°18'48.054", 5°9'35.655") showed a temperature of 11.8 °C and a salinity of 31.1 on 14 May 2019.

Sample No.	Time [UTC]	Day May	Lat. [°N]	Lon. [°E]	Temp [°C]	Sal [PSU]	TA / DIC [µmol kg⁻¹]	Si / NO_3^- [µmol L⁻¹]	Ca / Ar [Ω]	pH
535	07:56	20	53.18	5.4	14.72	30.24	2507 / 2357	10.00 / 5.10	3.0 / 1.9	7.92
536	08:26	20	53.19	5.34	14.81	32.51	2458 / 2296	3.45 / 0.46	3.1 / 2.0	7.92
537	08:53	20	53.22	5.29	14.05	32.38	2413 / 2227	1.92 / 0.85	3.4 / 2.2	8.00
538	09:28	20	53.23	5.19	13.36	32.65	2381 / 2153	0.52 / 1.02	4.0 / 2.6	8.10
539	09:53	20	53.27	5.17	13.17	32.65	2389 / 2161	0.45 / 1.37	4.0 / 2.6	8.10
540***	10:36	20	53.33	5.12	12.77	32.97	2375 / 2118	0.32 / 0.84	4.4 / 2.8	8.16
541	11:03	20	53.32	5.0	12.41	33.25	2368 / 2097	0.34 / 0.77	4.6 / 3.0	8.19
542**	11:49	20	53.4	5.1	12.93	32.92	2374 / 2109	0.44 / 0.81	4.6 / 2.9	8.17
543	12:49	20	53.45	5.33	12.95	32.45	2385 / 2196	6.25 / 1.85	3.4 / 2.2	8.02
544	13:31	20	53.46	5.5	13.55	32.51	2388 / 2169	3.02 / 1.30	3.9 / 2.5	8.08
558	11:33	22	53.41	5.65	13.31	32.51	2384 / 2224	2.57 / 1.56	3.0 / 1.9	7.95
559	12:04	22	53.4	5.66	13.45	32.51	2393 / 2195	1.58 / 1.41	3.6 / 2.3	8.03
560	12:40	22	53.39	5.69	13.67	32.52	2391 / 2183	1.52 / 1.33	3.7 / 2.4	8.05
561	13:09	22	53.4	5.73	14.23	32.48	2418 / 2242	2.04 / 1.04	3.3 / 2.1	7.97
562	13:32	22	53.42	5.77	14.71	32.51	2417 / 2237	3.23 / 1.04	3.3 / 2.1	7.97

563*	13:56	22	53.42	5.82	15.33	32.45	2421 / 2242	4.68 / 0.86	3.3 / 2.1	7.96
579	09:05	24	53.42	5.77	15.26	32.65	2417 / 2215	2.71 / 0.86	3.7 / 2.4	8.01
580	09:31	24	53.4	5.73	14.99	32.66	2426 / 2249	3.52 / 1.46	3.3 / 2.1	7.95
581	10:01	24	53.4	5.66	13.87	32.58	2396 / 2205	1.69 / 1.60	3.5 / 2.2	8.01
582	10:25	24	53.43	5.61	14.36	32.51	2389 / 2193	2.23 / 2.52	3.6 / 2.3	8.02
583	10:59	24	53.5	5.61	13.48	32.58	2382 / 2187	3.69 / 3.41	3.5 / 2.2	8.03
584	11:31	24	53.51	5.76	13.50	32.59	2390 / 2172	1.93 / 2.96	3.9 / 2.5	8.07
585	12:00	24	53.52	5.9	13.65	32.59	2390 / 2173	2.34 / 2.23	3.9 / 2.5	8.07
586	12:30	24	53.52	6.04	13.50	32.48	2384 / 2179	2.00 / 1.53	3.7 / 2.3	8.05
587	13:02	24	53.45	6.07	15.13	32.40	2389 / 2169	0.70 / 1.19	3.9 / 2.5	8.05
588	13:31	24	53.42	6.38	15.63	31.96	2396 / 2182	1.33 / 0.62	3.9 / 2.5	8.04
589	07:20	25	53.42	6.18	15.73	28.31	2430 / 2245	4.16 / 5.13	3.6 / 2.3	8.02
590	07:52	25	53.44	6.09	15.80	30.90	2407 / 2225	1.58 / 1.39	3.4 / 2.2	7.98
591	08:21	25	53.48	6.08	15.34	31.82	2395 / 2222	4.16 / 5.09	3.3 / 2.1	7.96
592	08:51	25	53.52	6.05	14.80	32.41	2386 / 2178	0.71 / 0.67	3.8 / 2.4	8.04
593	09:22	25	53.55	6.18	13.96	32.30	2379 / 2175	0.36 / 1.52	3.7 / 2.3	8.04
594	09:53	25	53.58	6.31	13.43	32.14	2332 / 2148	0.34 / 5.75	3.3 / 2.1	8.01
595	10:24	25	53.61	6.45	13.47	32.10	2347 / 2113	0.26 / 5.19	4.1 / 2.6	8.12
596	11:05	25	53.58	6.63	14.50	29.99	2381 / 2184	0.78 / 20.25	3.7 / 2.3	8.05
597	11:33	25	53.52	6.75	14.94	29.17	2383 / 2214	3.04 / 27.84	3.3 / 2.1	7.99
598	12:00	25	53.47	6.85	15.28	27.82	2395 / 2249	8.90 / 37.93	3.0 / 1.9	7.94
599	12:30	25	53.4	6.95	15.46	26.39	2423 / 2284	17.63 / 36.54	2.9 / 1.8	7.94
600	12:59	25	53.33	7.02	15.76	23.01	2460 / 2343	41.93 / 37.68	2.7 / 1.7	7.92
601	13:29	25	53.33	7.16	15.96	20.25	2517 / 2430	56.32 / 37.94	2.3 / 1.4	7.86

454

Data availability

456 The data of this study are presented in the appendices of this article or are available upon request from the corresponding
457 author.

Author Contributions

MN wrote the manuscript, did the carbon sampling and sample measurement, analyzed and evaluated the data, and led the study. JvB led the research cruise. JvB and HT contributed with editorial and scientific recommendations. MN prepared the manuscript with contribution from all co-authors.

Competing interests

The contact author has declared that none of the authors has any competing interests.

Acknowledgement

We thank the crew from RV *Ludwig Prandtl* for their support during the cruise. We thank Leon Schmidt for the nutrient sampling and measurements, and Marc Metzke for the C/N measurements, and Yoana Voynova and her department for the FerryBox preparation. We further thank the Editor and two anonymous reviewers for their constructive comments, which greatly improved this manuscript.

Financial support

This research has been funded by the German Academic Exchange Service (DAAD, project: MOPGA-GRI, grant no. 57429828), which received funds from the German Federal Ministry of Education and Research (BMBF).

References

Abril, G., and Frankignoulle, M.: Nitrogen–alkalinity interactions in the highly polluted Scheldt basin (Belgium), Water Research, 35, 844-850, https://doi.org/10.1016/S0043-1354(00)00310-9, 2001.

Beck, M., Dellwig, O., Holstein, J. M., Grunwald, M., Liebezeit, G., Schnetger, B., and Brumsack, H.-J.: Sulphate, dissolved organic carbon, nutrients and terminal metabolic products in deep pore waters of an intertidal flat, Biogeochemistry, 89, 221-238, https://doi.org/10.1007/s10533-008-9215-6, 2008a.

Beck, M., Dellwig, O., Liebezeit, G., Schnetger, B., and Brumsack, H.-J.: Spatial and seasonal variations of sulphate, dissolved organic carbon, and nutrients in deep pore waters of intertidal flat sediments, Estuarine, Coastal and Shelf Science, 79, 307-316, https://doi.org/10.1016/j.ecss.2008.04.007, 2008b.

Berner, R. A., Scott, M. R., and Thomlinson, C.: Carbonate alkalinity in the pore waters of anoxic marine sediments 1, Limnology and Oceanography, 15, 544-549, https://doi.org/10.4319/lo.1970.15.4.0544, 1970.

Berner, R. A., Lasaga, A. C., and Garrels, R. M.: Carbonate-silicate geochemical cycle and its effect on atmospheric carbon dioxide over the past 100 million years, Am. J. Sci.;(United States), 283, doi:10.2475/ajs.283.7.641., 1983.

Billerbeck, M., Werner, U., Polerecky, L., Walpersdorf, E., DeBeer, D., and Huettel, M.: Surficial and deep pore water circulation governs spatial and temporal scales of nutrient recycling in intertidal sand flat sediment, Marine Ecology Progress Series, 326, 61-76, 2006.

Borges, A. V., Delille, B., and Frankignoulle, M.: Budgeting sinks and sources of CO_2 in the coastal ocean: Diversity of ecosystems counts, Geophysical research letters, 32, doi.org/10.1029/2005GL023053, 2005.

Bozec, Y., Thomas, H., Elkalay, K., and de Baar, H. J.: The continental shelf pump for CO_2 in the North Sea—evidence from summer observation, Marine Chemistry, 93, 131-147, https://doi.org/10.1016/j.marchem.2004.07.006, 2005.

Brasse, S., Reimer, A., Seifert, R., and Michaelis, W.: The influence of intertidal mudflats on the dissolved inorganic carbon and total alkalinity distribution in the German Bight, southeastern North Sea, Journal of Sea Research, 42, 93-103, 1999.

Brenner, H., Braeckman, U., Le Guitton, M., and Meysman, F. J.: The impact of sedimentary alkalinity release on the water column CO_2 system in the North Sea, Biogeosciences, 13, 841-863, https://doi.org/10.5194/bg-13-841-2016, 2016.

Brewer, P. G., and Goldman, J. C.: Alkalinity changes generated by phytoplankton growth, Limnology and Oceanography, 21, 108-117, https://doi.org/10.4319/lo.1976.21.1.0108, 1976.

Brzezinski, M. A.: The Si: C: N ratio of marine diatoms: interspecific variability and the effect of some environmental variables, Journal of Phycology, 21, 347-357, https://doi.org/10.1111/j.0022-3646.1985.00347.x, 1985.

Burchard, H., Flöser, G., Staneva, J. V., Badewien, T. H., and Riethmüller, R.: Impact of density gradients on net sediment transport into the Wadden Sea, Journal of Physical Oceanography, 38, 566-587, 2008.

Burt, W., Thomas, H., Hagens, M., Pätsch, J., Clargo, N., Salt, L., Winde, V., and Böttcher, M.: Carbon sources in the North Sea evaluated by means of radium and stable carbon isotope tracers, Limnology and Oceanography, 61, 666-683, https://doi.org/10.1002/lno.10243, 2016.

Carter, B. R., Toggweiler, J., Key, R. M., and Sarmiento, J. L.: Processes determining the marine alkalinity and calcium carbonate saturation state distributions, Biogeosciences, 11, 7349-7362, https://doi.org/10.5194/bg-11-7349-2014, 2014.

Charalampopoulou, A., Poulton, A. J., Tyrrell, T., and Lucas, M. I.: Irradiance and pH affect coccolithophore community composition on a transect between the North Sea and the Arctic Ocean, Marine Ecology Progress Series, 431, 25-43, https://doi.org/10.3354/meps09140, 2011.

Chen, C. T. A., and Wang, S. L.: Carbon, alkalinity and nutrient budgets on the East China Sea continental shelf, Journal of Geophysical Research: Oceans, 104, 20675-20686, https://doi.org/10.1029/1999JC900055, 1999.

Crutzen, P.: Geology of mankind, Nature, 415, https://doi.org/10.1038/415023a, 2002.

De Beer, D., Wenzhöfer, F., Ferdelman, T. G., Boehme, S. E., Huettel, M., van Beusekom, J. E., Böttcher, M. E., Musat, N., and Dubilier, N.: Transport and mineralization rates in North Sea sandy intertidal sediments, Sylt-Rømø basin, Wadden Sea, Limnology and Oceanography, 50, 113-127, 2005.

De Jonge, V., Essink, K., and Boddeke, R.: The Dutch Wadden Sea: a changed ecosystem, Hydrobiologia, 265, 45-71, https://doi.org/10.1007/BF00007262, 1993.

Dickson, A., and Millero, F. J.: A comparison of the equilibrium constants for the dissociation of carbonic acid in seawater media, Deep Sea Research Part A. Oceanographic Research Papers, 34, 1733-1743, https://doi.org/10.1016/0198-0149(87)90021-5, 1987.

Dickson, A. G.: An exact definition of total alkalinity and a procedure for the estimation of alkalinity and total inorganic carbon from titration data, Deep Sea Research Part A. Oceanographic Research Papers, 28, 609-623, https://doi.org/10.1016/0198-0149(81)90121-7, 1981.

Duran-Matute, M., Gerkema, T., De Boer, G., Nauw, J., and Gräwe, U.: Residual circulation and freshwater transport in the Dutch Wadden Sea: a numerical modelling study, Ocean Science, 10, 611-632, 2014.

Elias, E. P., Van der Spek, A. J., Wang, Z. B., and De Ronde, J.: Morphodynamic development and sediment budget of the Dutch Wadden Sea over the last century, Netherlands Journal of Geosciences, 91, 293-310, https://doi.org/10.1017/S0016774600000457, 2012.

Faber, P. A., Evrard, V., Woodland, R. J., Cartwright, I. C., and Cook, P. L.: Pore-water exchange driven by tidal pumping causes alkalinity export in two intertidal inlets, Limnology and Oceanography, 59, 1749-1763, https://doi.org/10.4319/lo.2014.59.5.1749, 2014.

Friedlingstein, P., O'sullivan, M., Jones, M. W., Andrew, R. M., Gregor, L., Hauck, J., Le Quéré, C., Luijkx, I. T., Olsen, A., and Peters, G. P.: Global carbon budget 2022, Earth System Science Data, 14, 4811-4900, 2022.

Glavovic, B., Limburg, K., Liu, K., Emeis, K., Thomas, H., Kremer, H., Avril, B., Zhang, J., Mulholland, M., and Glaser, M.: Living on the Margin in the Anthropocene: engagement arenas for sustainability research and action at the ocean–land interface, Current Opinion in Environmental Sustainability, 14, 232-238, https://doi.org/10.1016/j.cosust.2015.06.003, 2015.

Grasshoff, K., Kremling, K., and Ehrhardt, M.: Methods of seawater analysis, John Wiley & Sons, 2009.

Hansen, H., and Koroleff, F.: Determination of nutrients. Methods of Seawater Analysis: Third, Completely Revised and Extended Edition. Grasshoff, K., Kremling, K., and Ehrhardt, M. (Eds.), Weinheim, Germany: Wiley-VCH Verlag GmbH, 2007.

Hickel, W.: Seston in the Wadden Sea of Sylt (German Bight, North Sea), Netherlands Institute for Sea Research - Publication Series, 10, 113-131, 1984.

Hoppema, J.: The distribution and seasonal variation of alkalinity in the southern bight of the North Sea and in the western Wadden Sea, Netherlands journal of sea research, 26, 11-23, https://doi.org/10.1016/0077-7579(90)90053-J, 1990.

Hoppema, J.: The oxygen budget of the western Wadden Sea, The Netherlands, Estuarine, Coastal and Shelf Science, 32, 483-502, https://doi.org/10.1016/0272-7714(91)90036-B, 1991.

Hoppema, J.: Carbon dioxide and oxygen disequilibrium in a tidal basin (Dutch Wadden Sea), Netherlands journal of sea research, 31, 221-229, https://doi.org/10.1016/0077-7579(93)90023-L, 1993.

Hu, X., and Cai, W. J.: An assessment of ocean margin anaerobic processes on oceanic alkalinity budget, Global Biogeochemical Cycles, 25, doi.org/10.1029/2010GB003859, 2011.

Huettel, M., Røy, H., Precht, E., and Ehrenhauss, S.: Hydrodynamical impact on biogeochemical processes in aquatic sediments, The Interactions between Sediments and Water: Proceedings of the 9th International Symposium on the Interactions between Sediments and Water, held 5–10 May 2002 in Banff, Alberta, Canada, 2003, 231-236,

Jahnke, R. A., Craven, D. B., and Gaillard, J.-F.: The influence of organic matter diagenesis on $CaCO_3$ dissolution at the deep-sea floor, Geochimica et Cosmochimica Acta, 58, 2799-2809, 1994.

Jensen, K., Jensen, M., and Kristensen, E.: Nitrification and denitrification in Wadden Sea sediments (Königshafen, Island of Sylt, Germany) as measured by nitrogen isotope pairing and isotope dilution, Aquatic Microbial Ecology, 11, 181-191, doi:10.3354/ame011181, 1996.

Keith, D. W., Ha-Duong, M., and Stolaroff, J. K.: Climate strategy with CO_2 capture from the air, Climatic Change, 74, 17-45, https://doi.org/10.1007/s10584-005-9026-x, 2006.

Kérouel, R., and Aminot, A.: Fluorometric determination of ammonia in sea and estuarine waters by direct segmented flow analysis, Marine Chemistry, 57, 265-275, https://doi.org/10.1016/S0304-4203(97)00040-6, 1997.

Kieskamp, W. M., Lohse, L., Epping, E., and Helder, W.: Seasonal variation in denitrification rates and nitrous oxide fluxes in intertidal sediments of the western Wadden Sea, Marine ecology progress series. Oldendorf, 72, 145-151, 1991.

Lewis, E., and Wallace, D.: Program developed for CO_2 system calculations, Environmental System Science Data Infrastructure for a Virtual Ecosystem, 1998.

Louters, T., and Gerritsen, F.: The Riddle of the Sands: A Tidal SystenVs Answer to a Rising Sea Level, report RIKZ-94.040 (isbn 90-369-0084-0), 1994.

Luff, R., and Moll, A.: Seasonal dynamics of the North Sea sediments using a three-dimensional coupled sediment–water model system, Continental Shelf Research, 24, 1099-1127, https://doi.org/10.1016/j.csr.2004.03.010, 2004.

Matthews, H. D., and Caldeira, K.: Stabilizing climate requires near-zero emissions, Geophysical research letters, 35, https://doi.org/10.1029/2007GL032388, 2008.

Mehrbach, C., Culberson, C., Hawley, J., and Pytkowicx, R.: Measurement of the apparent dissociation constants of carbonic acid in seawater at atmospheric pressure, Limnology and oceanography, 18, 897-907, https://doi.org/10.4319/lo.1973.18.6.0897, 1973.

Meybeck, M.: Global chemical weathering of surficial rocks estimated from river dissolved loads, American journal of science, 287, 401-428, 10.2475/ajs.287.5.401, 1987.

Middelburg, J. J., Soetaert, K., and Hagens, M.: Ocean alkalinity, buffering and biogeochemical processes, Reviews of Geophysics, 58, e2019RG000681, https://doi.org/10.1029/2019RG000681, 2020.

Millero, F. J., Byrne, R. H., Wanninkhof, R., Feely, R., Clayton, T., Murphy, P., and Lamb, M. F.: The internal consistency of CO_2 measurements in the equatorial Pacific, Marine Chemistry, 44, 269-280, 1993.

Norbisrath, M., Pätsch, J., Dähnke, K., Sanders, T., Schulz, G., van Beusekom, J. E., and Thomas, H.: Metabolic alkalinity release from large port facilities (Hamburg, Germany) and impact on coastal carbon storage, Biogeosciences, 19, 5151-5165, https://doi.org/10.5194/bg-19-5151-2022, 2022.

Norbisrath, M., Neumann, A., Dähnke, K., Sanders, T., Schöl, A., van Beusekom, J. E., and Thomas, H.: Alkalinity and nitrate dynamics reveal dominance of anammox in a hyper-turbid estuary, Biogeosciences, 20, 4307–4321, https://doi.org/10.5194/bg-20-4307-2023, 2023.

Orr, J. C., Epitalon, J.-M., Dickson, A. G., and Gattuso, J.-P.: Routine uncertainty propagation for the marine carbon dioxide system, Marine Chemistry, 207, 84-107, 2018.

Pätsch, J.: Daily Loads of Nutrients, Total Alkalinity, Dissolved Inorganic Carbon and Dissolved Organic Carbon of the European Continental Rivers for the Years 1977 – 2022. 2024.

Petersen, W., Schroeder, F., and Bockelmann, F.-D.: FerryBox-Application of continuous water quality observations along transects in the North Sea, Ocean Dynamics, 61, 1541-1554, https://doi.org/10.1007/s10236-011-0445-0, 2011.

Postma, H.: Hydrography of the Dutch Wadden sea, Arch. Neerl. Zool, 10, 405-511, 1954.

Renforth, P., and Henderson, G.: Assessing ocean alkalinity for carbon sequestration, Reviews of Geophysics, 55, 636-674, https://doi.org/10.1002/2016RG000533, 2017.

Ridderinkhof, H., Zimmerman, J., and Philippart, M.: Tidal exchange between the North Sea and Dutch Wadden Sea and mixing time scales of the tidal basins, Netherlands Journal of Sea Research, 25, 331-350, https://doi.org/10.1016/0077-7579(90)90042-F, 1990.

Røy, H., Lee, J. S., Jansen, S., and de Beer, D.: Tide-driven deep pore-water flow in intertidal sand flats, Limnology and oceanography, 53, 1521-1530, https://doi.org/10.4319/lo.2008.53.4.1521, 2008.

Rutgers van der Loeff, M.: Transport van reactief silikaat uit Waddenzee sediment naar het bovenstaande water, NIOZ-rapport, 1974.

Sabine, C. L., Feely, R. A., Gruber, N., Key, R. M., Lee, K., Bullister, J. L., Wanninkhof, R., Wong, C., Wallace, D. W., and Tilbrook, B.: The oceanic sink for anthropogenic CO_2, science, 305, 367-371, DOI: 10.1126/science.1097403, 2004.

Santos, I. R., Chen, X., Lecher, A. L., Sawyer, A. H., Moosdorf, N., Rodellas, V., Tamborski, J., Cho, H.-M., Dimova, N., and Sugimoto, R.: Submarine groundwater discharge impacts on coastal nutrient biogeochemistry, Nature Reviews Earth & Environment, 2, 307-323, https://doi.org/10.1038/s43017-021-00152-0, 2021.

Schwichtenberg, F., Callies, U., and van Beusekom, J. E.: Residence times in shallow waters help explain regional differences in Wadden Sea eutrophication, Geo-Marine Letters, 37, 171-177, https://doi.org/10.1007/s00367-016-0482-2, 2017.

Schwichtenberg, F., Pätsch, J., Böttcher, M. E., Thomas, H., Winde, V., and Emeis, K.-C.: The impact of intertidal areas on the carbonate system of the southern North Sea, Biogeosciences, 17, 4223-4245, https://doi.org/10.5194/bg-17-4223-2020, 2020.

Shadwick, E., Thomas, H., Gratton, Y., Leong, D., Moore, S., Papakyriakou, T., and Prowe, A.: Export of Pacific carbon through the Arctic Archipelago to the North Atlantic, Continental Shelf Research, 31, 806-816, https://doi.org/10.1016/j.csr.2011.01.014, 2011.

Suchet, P. A., and Probst, J.-L.: Modelling of atmospheric CO_2 consumption by chemical weathering of rocks: application to the Garonne, Congo and Amazon basins, Chemical Geology, 107, 205-210, DOI:10.1016/0009-2541(93)90174-H, 1993.

Thomas, H., Bozec, Y., Elkalay, K., and De Baar, H. J.: Enhanced open ocean storage of CO_2 from shelf sea pumping, Science, 304, 1005-1008, DOI: 10.1126/science.1095491, 2004.

Thomas, H., Schiettecatte, L.-S., Suykens, K., Koné, Y., Shadwick, E., Prowe, A. F., Bozec, Y., de Baar, H. J., and Borges, A.: Enhanced ocean carbon storage from anaerobic alkalinity generation in coastal sediments, Biogeosciences, 6, 267-274, https://doi.org/10.5194/bg-6-267-2009, 2009.

van Bennekom, A., Krijgsman-van Hartingsveld, E., van der Veer, G., and van Voorst, H.: The seasonal cycles of reactive silicate and suspended diatoms in the Dutch Wadden Sea, Netherlands Journal of Sea Research, 8, 174-207, https://doi.org/10.1016/0077-7579(74)90016-7, 1974.

van Beusekom, J., Brockmann, U., Hesse, K.-J., Hickel, W., Poremba, K., and Tillmann, U.: The importance of sediments in the transformation and turnover of nutrients and organic matter in the Wadden Sea and German Bight, Deutsche Hydrografische Zeitschrift, 51, 245-266, 10.1007/BF02764176, 1999.

van Beusekom, J., and De Jonge, V.: Long-term changes in Wadden Sea nutrient cycles: importance of organic matter import from the North Sea, in: Nutrients and Eutrophication in Estuaries and Coastal Waters, Springer, 185-194, 2002.

van Beusekom, J. E., Buschbaum, C., and Reise, K.: Wadden Sea tidal basins and the mediating role of the North Sea in ecological processes: scaling up of management?, Ocean & coastal management, 68, 69-78, https://doi.org/10.1016/j.ocecoaman.2012.05.002, 2012.

van Beusekom, J. E., Carstensen, J., Dolch, T., Grage, A., Hofmeister, R., Lenhart, H., Kerimoglu, O., Kolbe, K., Pätsch, J., and Rick, J.: Wadden Sea Eutrophication: long-term trends and regional differences, Frontiers in Marine Science, 6, 370, doi.org/10.3389/fmars.2019.00370, 2019.

van der Zee, C., and Chou, L.: Seasonal cycling of phosphorus in the Southern Bight of the North Sea, Biogeosciences, 2, 27-42, https://doi.org/10.5194/bg-2-27-2005, 2005.

van Raaphorst, W., and van der Veer, H. W.: The phosphorus budget of the Marsdiep tidal basin (Dutch Wadden Sea) in the period 1950–1985: importance of the exchange with the North Sea, in: North Sea—Estuaries Interactions, Springer, 21-38, 1990.

Voynova, Y. G., Petersen, W., Gehrung, M., Aßmann, S., and King, A. L.: Intertidal regions changing coastal alkalinity: The Wadden Sea-North Sea tidally coupled bioreactor, Limnology and Oceanography, 64, 1135-1149, 2019.

Wang, Z. A., Kroeger, K. D., Ganju, N. K., Gonneea, M. E., and Chu, S. N.: Intertidal salt marshes as an important source of inorganic carbon to the coastal ocean, Limnology and Oceanography, 61, 1916-1931, 2016.

Waska, H., and Kim, G.: Submarine groundwater discharge (SGD) as a main nutrient source for benthic and water-column primary production in a large intertidal environment of the Yellow Sea, Journal of Sea Research, 65, 103-113, https://doi.org/10.1016/j.seares.2010.08.001, 2011.

Wolf-Gladrow, D. A., Zeebe, R. E., Klaas, C., Körtzinger, A., and Dickson, A. G.: Total alkalinity: The explicit conservative expression and its application to biogeochemical processes, Marine Chemistry, 106, 287-300, https://doi.org/10.1016/j.marchem.2007.01.006, 2007.

Wu, Z., Zhou, H., Zhang, S., and Liu, Y.: Using ^{222}Rn to estimate submarine groundwater discharge (SGD) and the associated nutrient fluxes into Xiangshan Bay, East China Sea, Marine pollution bulletin, 73, 183-191, https://doi.org/10.1016/j.marpolbul.2013.05.024, 2013.

Zalasiewicz, J., Williams, M., Steffen, W., and Crutzen, P.: The new world of the Anthropocene. ACS Publications, 2010.

Zhang, C., Shi, T., Liu, J., He, Z., Thomas, H., Dong, H., Rinkevich, B., Wang, Y., Hyun, J.-H., and Weinbauer, M.: Eco-engineering approaches for ocean negative carbon emission, Science Bulletin, 67, 2564-2573, https://doi.org/10.1016/j.scib.2022.11.016, 2022.